patterns of *OATP1B3* signatures in *OATP1B3*-high (blue box), *OATP1B3*-low AFP-low (<100 ng/mL) (orange box), and *OATP1B3*-low AFP-high (≥100 ng/mL; red box) after hierarchical clustering of genes and samples, shown as a heat map image. Red indicates a high expression level; green indicates a low expression level. *OATP1B3*-high HCCs and *OATP1B3*-low AFP-high HCCs were clustered in B1 (green bar) and B2 (yellow bar), respectively. (D) Representative expression of genes in clusters A (*KRT19*, *EPCAM*, and *MKI67*) and B (*OATP1B3*, *ALB*, and *CYP3A4*). The green and orange bars indicate HCCs clustered in B1 and B2, respectively. (E) The activated pathways are identified in clusters A (orange bar) and B (blue bar). (F) Genes encoding transcription factors activated or inactivated in *OATP1B3*-high HCCs.

Figure 2 Transcriptional programs of HCCs corresponding to the EOB-MRI findings and serum AFP.

(A, B) Scatter plot analyses of the microarray data of 238 HCCs. (C) Representative photomicrographs of IHC staining with anti-HNF4α, anti-FOXM1, and anti-Ki-67 antibodies in class A, B, and C HCCs, according to the EOB-AFP classification. (D) Ki-67 labeling index in class A, B, and C HCCs. (E) Summary of FOXM1 and HNF4α expression in class A, B, and C HCCs.

Figure 3 HNF4α regulates a mature hepatocyte-like, less aggressive HCC phenotype coupled with Gd-EOB-DTPA uptake in hyper-intense HCC.

(A) MRI scans of hyper-intense (a) and hypo-intense (b) HCCs in the hepatobiliary phase before surgery. The T/N signal intensity ratios of the images in the hepatobiliary phase were 1.02 (left panel) and 0.49 (right panel). Surgically resected specimens were subsequently used for mouse

xenotransplantation. (B) MRI scans of NOD/SCID mouse xenotransplanted with hyper-intense (a) and hypo-intense (b) HCCs in the hepatobiliary phase. The T/N signal intensity ratios of the images were 0.82 (upper panel) and 0.45 (lower panel). (C) Left panel: Expression of HNF4α protein by western blotting. Hyper-intense HCC cells were harvested in dishes and treated with retroviruses encoding an expression cassette against *HNF4A* (Sh-HNF4A) or scramble sequence (Sh-Scr). Right panel: qRT-PCR of *AFP*, *FOXM1*, *CYP3A4*, and *OATP1B3* in hyper-intense HCC cells transfected with Sh-Scr or Sh-HNF4A. (D) Left panel: Immunofluorescence analysis of HNF4α (red) and OATP1B3 (green) in hyper-intense HCC cells transfected with Sh-Scr or Sh-HNF4A (scale bar, 100 μm). Right panel: Representative photomicrographs of hyper-intense HCC cells transfected with Sh-Scr or Sh-HNF4A (scale bar, 100 μm). (E) MRI scans of NOD/SCID mouse xenotransplanted with hyper-intense HCC cells transfected with Sh-Scr (day 49 after transplantation) or Sh-HNF4A (day 43 after transplantation). The T/N signal intensity ratios of the images in the hepatobiliary phase were 0.65 (left panel) and 0.34 (right panel). (F) Survival of NOD/SCID mice xenotransplanted with hyper-intense HCC cells transfected with Sh-Scr (n = 5) or Sh-HNF4A (n = 5).

Figure 4 Prognostic utility of the EOB-AFP classification.

(A, B) Overall survival curves of Cohorts 1 (A) and 2 (B). (C, D) Overall survival curves of Cohorts 1 (C) and 2 (D) according to the EOB-AFP classification. (E) The EOB-AFP classification system and its molecular basis.

Acknowledgments

We thank Drs. Yutaka Aoyagi (Division of Gastroenterology and Hepatology, Niigata University Graduate School of Medical and Dental Sciences, Niigata, Japan), Hiroko Iijima (Division of

Hepatobiliary and Pancreatic Disease, Department of Internal Medicine, Hyogo College of Medicine, Hyogo, Japan), and Michio Sata (Division of Gastroenterology, Department of Medicine, Kurume University School of Medicine, Kurume, Japan) for their help with patient enrollment. We also thank Mss. Masayo Baba and Nami Nishiyama for excellent technical assistance.

Table 1. Characteristics of HCCs classified by EOB-MRI in cohort 1 and 2

Characteristics	Cohort 1			Cohort 2		
	Hyper-intense (n = 9)	Hypo-intense (n = 61)	*P**	Hyper-intense (n = 9)	Hypo-intense (n = 100)	*P**
Age (years, mean ± SE)	66.2 ± 3.6	64.6 ± 1.2	0.21	67.2 ± 2.0	66.2 ± 1.0	1.0
Sex (male/female)	7/2	44/17	0.72	9/0	79/21	0.13
Etiology (HBV/HCV/other)	2/3/4	14/23/24	0.95	1/6/0/2	22/56/2/20	0.52
Liver cirrhosis (yes/no)	5/4	33/28	0.94	2/7	42/58	0.25
AFP (ng/mL, mean ± SE)	12.4 ± 1.9	2,157 ± 866	0.03	7.0 ± 2.2	188.4 ± 74	0.03
Histologic grade†						
I–II	1	12		2	16	
II–III	8	38		7	74	

III–IV	0	11	0.25	0	10	0.57
Tumor size (cm, mean ± SE)	4.0 ± 0.9	4.4 ± 0.4	0.79	3.3 ± 0.4	2.6 ± 0.1	0.09
Tumor number (single/multiple)	7/2	48/13	0.95	8/1	86/14	0.81
Macroscopic portal vein invasion (yes/no)	1/8	5/56	0.58	0/9	0/100	
Microscopic portal vein invasion (yes/no)	2/7	27/34	0.21	0/9	11/89	0.59
Tumor-node-metastasis classification (I/II/III)	6/2/1	29/28/4	0.40	7/2/0	75/25/0	0.85
BCLC stage (0/A/B/C)	0/7/1/1	4/30/22/5	0.34	0/9/0/0	27/73/0/0	0.07
Elapsed time between MRI and surgery (days, mean ± SE)	47.0 ± 8.4	51.5 ± 3.2	0.73	17.3 ± 5.0	20.6 ± 3.0	0.50

Surgical procedure (partial resection or segmentectomy/ lobectomy or extended lobectomy)	6/3	35/26	0.60	8/1	86/14	1.0

*Mann–Whitney test, Fisher's exact test or χ^2 test.
†Edmondson–Steiner.

Figure 1

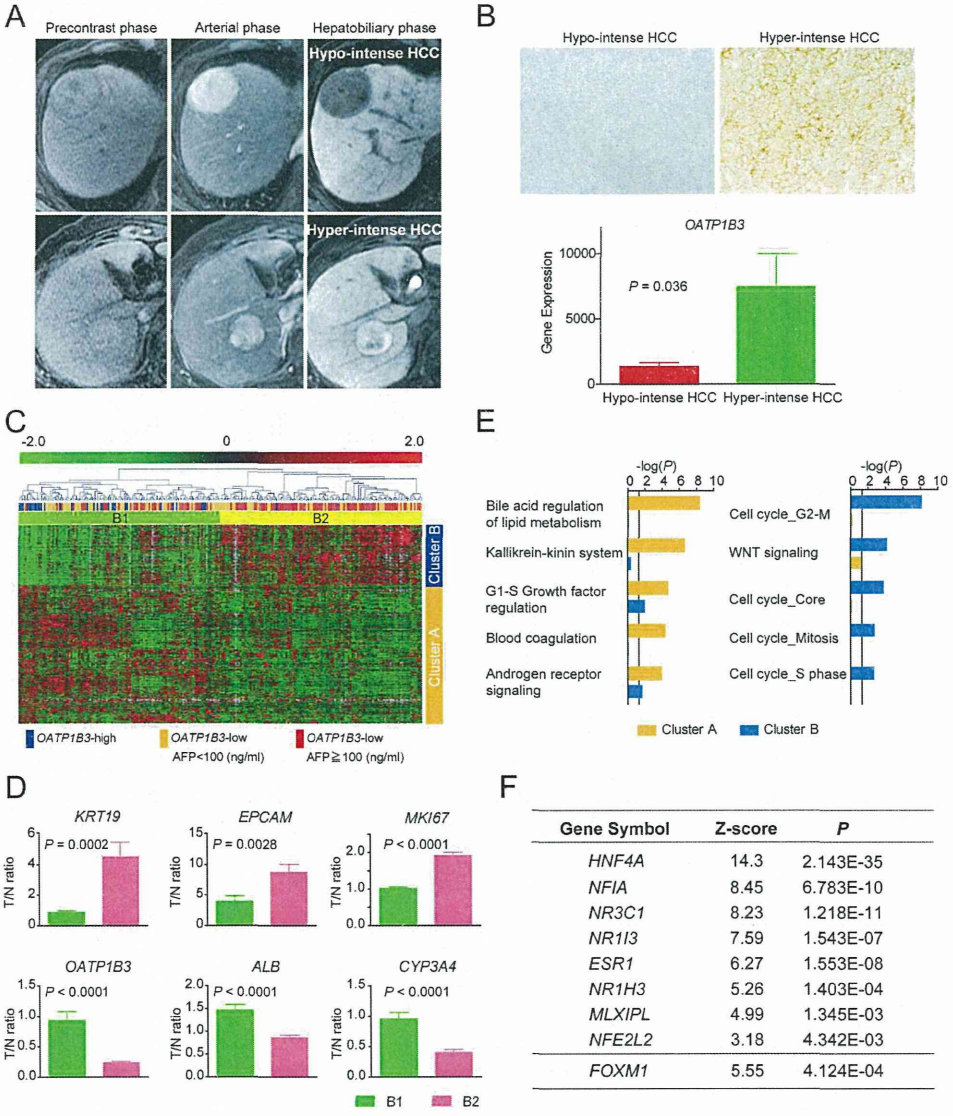

F

Gene Symbol	Z-score	*P*
HNF4A	14.3	2.143E-35
NFIA	8.45	6.783E-10
NR3C1	8.23	1.218E-11
NR1I3	7.59	1.543E-07
ESR1	6.27	1.553E-08
NR1H3	5.26	1.403E-04
MLXIPL	4.99	1.345E-03
NFE2L2	3.18	4.342E-03
FOXM1	5.55	4.124E-04

193x238mm (300 x 300 DPI)

Figure 2

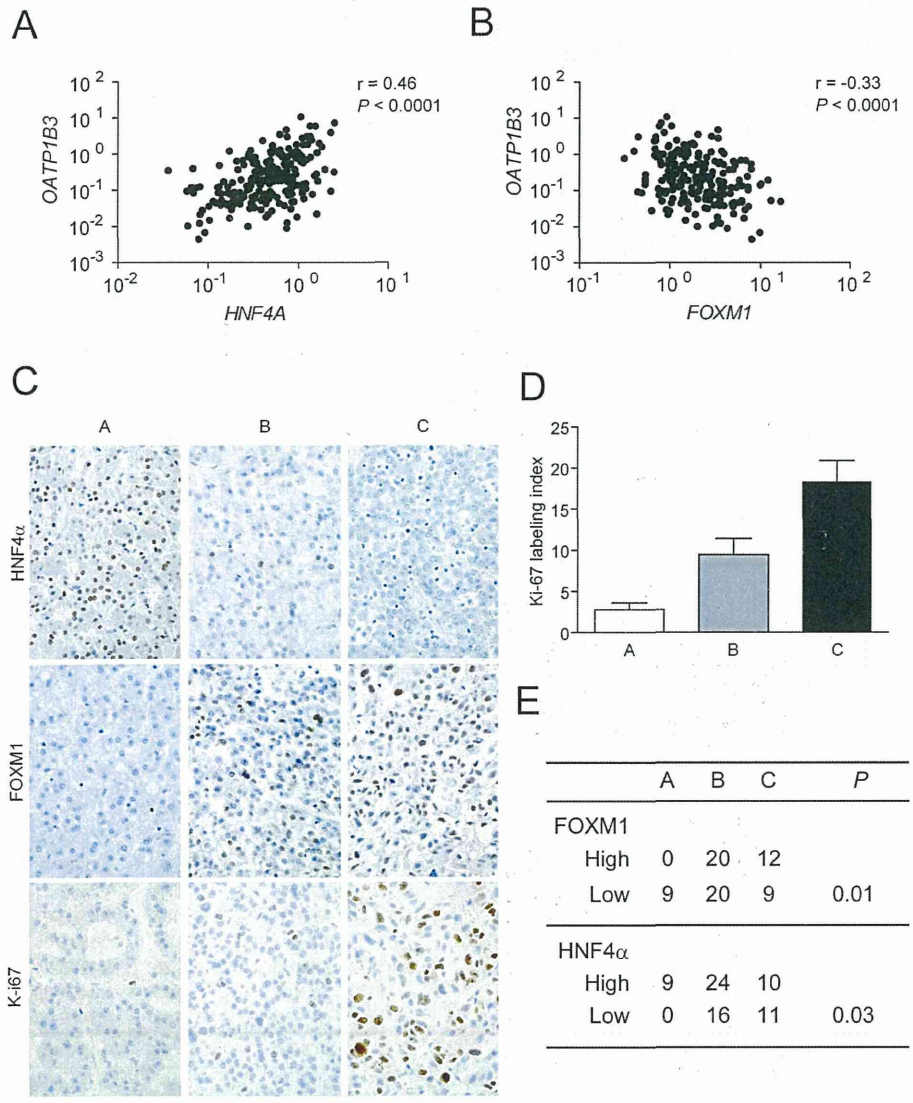

	A	B	C	*P*
FOXM1				
High	0	20	12	
Low	9	20	9	0.01
HNF4α				
High	9	24	10	
Low	0	16	11	0.03

149x186mm (300 x 300 DPI)

Figure 3

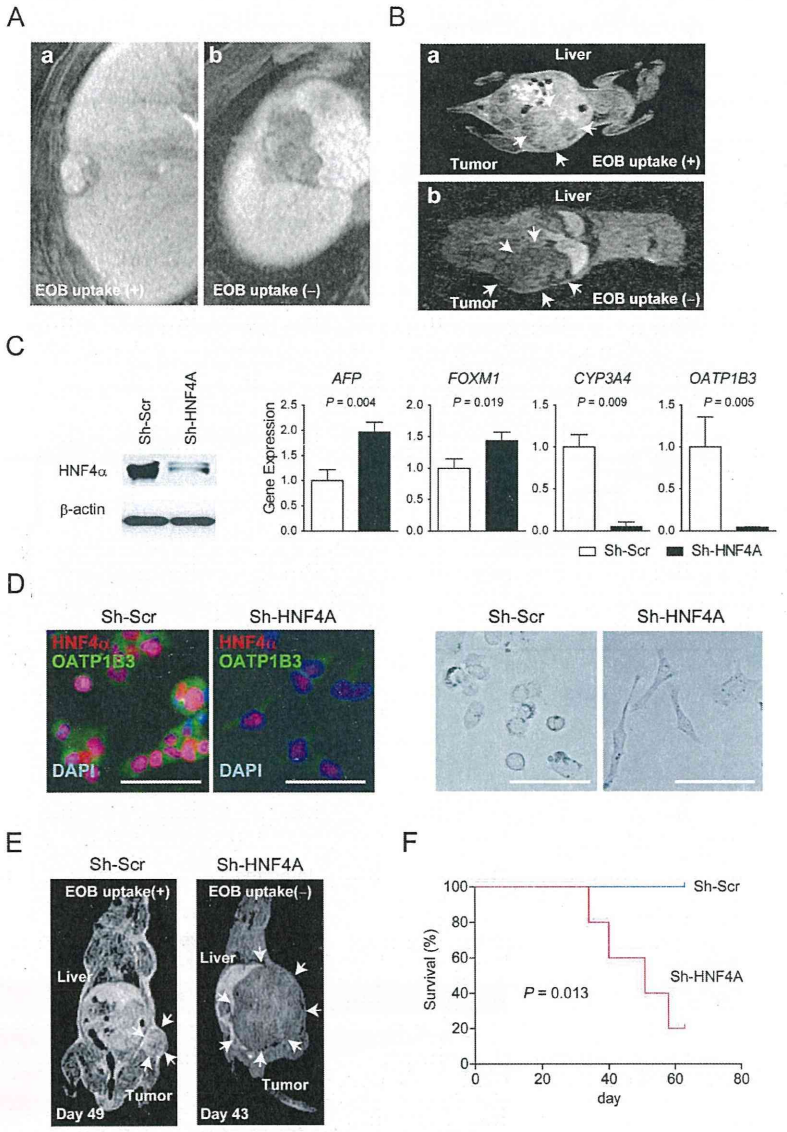

182x272mm (300 x 300 DPI)

Figure 4

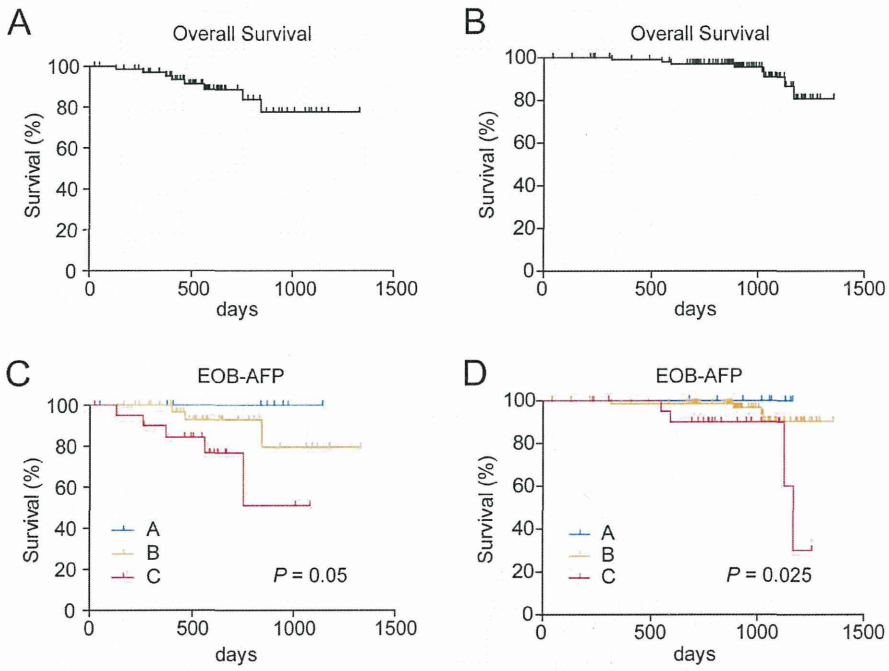

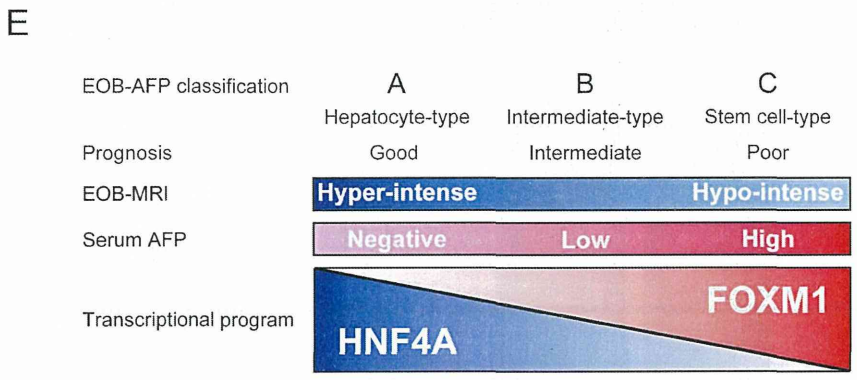

158x204mm (300 x 300 DPI)